SHAPE CONTEXT MATCHING FOR THE SELF-LOCALIZATION OF PLANETARY ROVER

Martin Lingenauber

Deutsches Zentrum für Luft- und Raumfahrt (DLR), Institut für Planetenforschung, Planetengeologie, Rutherfordstraße 2, 12489 Berlin, Germany, Email: martin@lingenauber.de

ABSTRACT

Future planetary rovers are expected to use their increased level of autonomy for traverses over several kilometres within one command cycle. Current on-board navigation concepts are limited to a range of approximately < 100 m per cycle, due to error accumulation. In order to overcome this limitation, a new self-localization procedure is proposed and described. It shall allow the determination of the absolute rover position within the planetary reference frame by registering a Digital Elevation Model (DEM), taken from a rover's point of view, to a DEM that is generated from orbiter image data.

As a proof of concept, an implementation of the DEM registration based on shape context descriptors was tested. For this, a detailed Mars surface was simulated to achieve the required orbiter- and rover DEMs with different levels of detail and different ground resolutions, respectively. The first tests of this basic implementation showed the conceptual feasibility with achieved matching ratios of up to 92.5 %.

1. INTRODUCTION

Future planetary rovers are expected to use their increased level of autonomy to achieve very long travel distances within one command cycle. Traverses of several kilometres for the Mars Science Laboratory are envisioned but also successful studies for over the horizon navigation were conducted [22]. Such a Very Long Distance Navigation (VLDN) requires new techniques that allow a precise and reliable self-localization within a large area to ensure the success of each traverse. Furthermore, the determination of the accurate absolute position of a rover within a Planetary Reference Frame (PRF) allows for a better consistency between rover data and data from other sources, e.g. orbiters.

Current on-board navigation systems are mainly based on relative navigation, i.e. the measured position and orientation are the result of an integration of single measurements of the movement from a starting point on. As a result, they are affected by the inherent error accumulation of measurement technologies such as wheel odometry, visual odometry or Inertial Measurement Units (IMU) [11]. Therefore, only short or medium distances (approximately < 100 m) are possible for autonomous navigation [16].

The landmark based localization provides a possible approach for long distance navigation by matching landmarks within the rover's Field Of View (FOV) with their corresponding representation in a reference data set (e.g. a map). From the combination of the position information of both data sets, the rover's position and orientation can be calculated. This form of localization is mostly independent from the observation conditions and as the surfaces of Moon and Mars are not affected by rapid changes, the requirements on the actuality of the reference data are relatively low. A possible implementation is proposed in [14]. An image network, consisting of overhead (orbital and descent) and rover image data shall be used for long distance navigation. The rover position is achieved through the reconstruction of the image pointing parameters [13]. Those result from an incremental bundle adjustment, which is used to compute the accurate 3D position of the tie points, at which the single images are stitched together. A tie point is a landmark feature such as hill peaks or rocks within the overlapping regions of the images. So far the landmarks are chosen by operators of the ground control team. Furthermore, in [12] an approach was introduced to find the rover position by registering an orthoimage, which was produced by a rover panoramic view, to an orbiter orthoimage. The deviation between the incremental bundle adjustment and the orthoimage method is approximately 0.1 % over a 7 km traverse [12].

1.1. Proposal of a new self-localization procedure with DEM-registration

To avoid the complexity of choosing suitable landmarks, a new self-localization procedure based on the matching of equally sized cut-outs from rover and orbiter Digital Elevation Models (DEM) is proposed in this work. It is assumed that each DEM cut-out, termed DEM patch, is unique in terms of its appearance in combination with its position within a larger area.

Reference data is available in terms of high resolution DEMs of the surface of Mars [8] and Moon [4], generated from orbiter image data as it was acquired e.g. by

the Mars Reconnaissance Orbiter or Mars Express. In the orbiter DEMs, the location of each pixel is known with respect to the applied PRF. The local data sets are provided as rover DEMs, which are created on-board of a rover, based on 3D image data from its stereo vision systems.

The DEM patches are regarded as 3D objects, hence the matching of a rover patch to an orbiter patch can be considered as a 3D object recognition. With help of a suitable descriptor, two catalogues with DEM patch descriptions, one for the orbiter patches and one for the rover patches, are created and used for the matching process. To ensure an efficient and reliable matching, the descriptions are required to be invariant against translation, rotation and scaling. Additionally, they shall be very robust against noise, against the resolution difference between the two DEMs and against large occluded areas that appear in the rover DEMs, due to the low elevation of the rover's stereo vision system.

One expected advantage of this approach is the re-utilization of already acquired data, hence the self-localization might be implemented as a software extension.

As a starting point of the development of the proposed procedure, this work is a first investigation of the capabilities of 3D Shape Context Matching (SCM), which was identified to be the most suitable approach for the matching of DEM patches (see section 3). For this a first, basic implementation of the SCM was created and tested in order to determine the quality of the matching strategy.

1.2. Paper outline

Section 2 covers the proposed self-localization procedure, along with a presentation of the available data sources and their properties. Furthermore, a set of requirements for the matching strategy was compiled to allow the identification of a suitable approach. Section 3 starts with a short overview of the available approaches and explains the choice for the Shape Context Matching. The introduction to Shape Contexts (SC) in section 3.1 is followed by the description of the SCM implementation that was used for this work. The experiments, which were used to show the feasibility of the SCM for the DEM-registration, are described in section 4, while the results are presented in section 5. Finally, the conclusion summarises the work.

2. SELF-LOCALIZATION WITH DEM-REGISTRATION

The goal of the proposed procedure is to register a rover DEM (target) with a georeferenced orbiter DEM (reference), in order to determine the rover's absolute position $\vec{p}_{abs}$ with respect to the PRF. By using the position information, contained in the rover-DEM, a rover might be able to localize itself.

As shown in Fig. 1, the position of a patch $P_a, a = 1 \ldots A \in \mathbb{N}$ in the orbiter DEM, is given in the orbiter DEM reference frame (global, upper index g) by the position vector $\vec{p}_a^{\,g}$. For the rover centred reference frame (local, upper index l), the position of P_a is given by $\vec{p}_a^{\,l}$. By combining the two position vectors, $\vec{p}_a^{\,g}$ and $\vec{p}_a^{\,l}$, with the position $\vec{p}_g$ of the orbiter DEM in the planetary reference frame, the absolute position $\vec{p}_{a,abs}$ of the rover based on patch P_a can be determined as

$$\vec{p}_{a,abs} = \vec{p}_g + \vec{p}_a^{\,o} + \vec{p}_a^{\,r} \tag{1}$$

The vectors $\vec{p}_a^{\,l}$ and $\vec{p}_a^{\,g}$ must be converted to the planetary reference system before the addition.

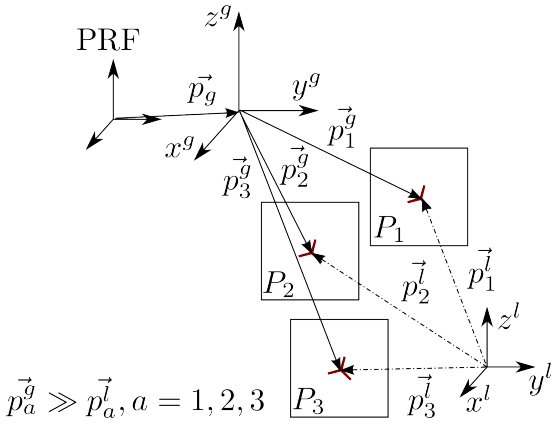

Figure 1: *Model of the proposed self-localization with matched DEM patches*

To enable this localization, a correct matching of the patch P_k from the orbiter DEM to its complement in the rover DEM is required. The limited elevation of the rover's camera point of view can lead to large occluded areas in the DEM, i.e. a spot-like feature could easily be occluded. A possibility to avoid this problem, would be to match patches large enough, that they are recognizable in both DEMs.

Regarding the extra complexity of the extraction of suitable objects from the DEMs, this method relies on DEM patches for matching. A patch is a large enough cut-out from the DEM, such that it can contain enough features by itself in order to allow a successful object recognition. Hence it is regarded to be a 3D object which can be described by its shape, in this case by its topography.

By choosing O patches from the orbiter DEM (global) and R patches from the rover DEM (local), with $O > R \gg 0$, it is expected to have a good chance that enough matches can be established for the position calculation. For each patch match, the absolute position $\vec{p}_{a,abs}$ of its centre is calculated with help of Eq. 1. In order to increase the accuracy of the position calculation, the average $\bar{\vec{p}}_{abs}$ of all calculated positions $\vec{p}_{a,abs}$ should be used as the final result of the position determination.

As the absolute Self-Localization (SL) is a supplement to the already existing, relative navigation systems on board of the rover, it shall be used in regular intervals, e.g. by

the end of a days traverse, to eliminate or reduce the accumulated navigation error. Depending on the current terrain, it might be necessary to perform an error calibration more often.

Each time the SL procedure is executed, a new rover catalogue with patch descriptions based on the actual rover DEM shall be created on board, followed by the matching with the patches from the orbiter catalogue. The orbiter catalogue is intended to be created beforehand on ground and it shall either be stored on-board the rover before launch or, depending on its size, it might be possible to upload it during the mission.

2.1. DEM data

Currently, the most suitable orbiter DEMs available are based on stereo image pairs from several orbits, as those data products offer the highest horizontal resolution (1 m pixel spacing). For Mars, DEMs based on images from Mars Express's HRSC camera are available with resolution between 10 and 30 m [8]. The Mars Reconnaissance Orbiter camera HiRISE provides images with up to 0.25 m ground resolution, resulting in DEMs with a resolution between 1 m and 2 m [24]. The DEMs are georeferenced, and in case of the HiRISE data aligned with the MOLA elevation model. The orbiter DEMs are raster data sets, hence their data points are equally distanced which results in an uniform, grid like sampling of the surface. For the Mars and Moon, a very slow erosion of the surface is assumed, i.e. the DEMs are not required to be based on actual image data.

The rover DEMs are processed from stereo image pairs taken by the navigation cameras. In case of the Mars Exploration Rovers (MER), the point of view is 1.5 m above ground and for the future Mars Science Laboratory (MSL) the cameras' elevation is approximately 2.3 m. As a result, obstacles in the rover's FOV can lead to occlusions in the resulting DEM. Because of the perspective of the stereo images, and in contrast to the orbiter DEMs, the surface is not sampled uniformly as more distant parts are covered by less pixels than closer parts. Furthermore, as a result of the usage of a stereo camera system, the ranging error of the DEM increases exponentially with the distance to the camera [17]. For the MER, the maximum range that can be covered with 1 m range accuracy is approximately 30 m [17].

2.2. Requirements for the matching procedure

As the orbiter patches are not necessarily aligned with the rover patches and as their might be differences in size and orientation, the patch descriptions are required to be invariant against translation, rotation and scaling. Additionally, they shall be robust against differences in the sampling distance, against resolution difference between the two DEMs and against large occluded areas that appear in the rover DEMs, due to the low elevation of the rover's stereo vision system. Furthermore, a catalogue of orbiter patches shall use less storage than the original DEM.

3. SHAPE CONTEXT MATCHING WITH DEMS

Due to the results of the survey about 3D shape retrieval methods in [23], descriptors based on the local feature similarity were identified to be the most suitable ones, as they are the only class providing partial matching capabilities (i.e. matching of occluded objects) for DEM-like data sets. Descriptors of this class describe an object based on its shape in the neighbourhood of sample points of a raster data set.

Currently, two different descriptors are available for the required DEM matching. Both use the vertexes of a meshed model for the object description. First, spin images [7] which are 2D images of the surface point locations around a basis point. For each basis point on an object's surface, the adjacent points are described as projections on a cylindrical coordinate system with its origin in the basis point. The resulting 2D spin-image describes the object's surface with respect to the basis point. By using several spin-images and comparing them to a reference set of spin-images, a 3D object recognition becomes possible.

Second, 3D SCs were developed by [9] as an extension of the 2D SC object recognition by [1]. SCs describe an object's surface with respect to a basis point. In contrast to spin-images, they use the distribution of the distance vectors to all neighbouring points in form of a histogram for the description (see 3). For the matching, the histograms are regarded as feature vectors which allows to measure their similarity based on their distance in the feature space.

Ref. [6] compared spin images, shape contexts and harmonic shape contexts for object recognition in heavily cluttered scenes based on laser range image data. Because of the their invariance against translation, scaling and rotation as well as due to their high robustness against occlusions, the SC descriptor showed the best matching ratios.

Therefore, SCM was chosen to be the best current approach for the challenge of DEM-registration within the proposed SL framework for planetary rovers.

3.1. 3D Shape Contexts

Shape Contexts are rich point descriptors that were developed by [2] for shape-based recognition of 2D objects. Extensions for 3D object recognition were developed by [9] and [6], where the latter successfully showed the recognition of heavily occluded objects in laser range image data.

SCs describe an object based on its shape by exploiting the relative distances between points on the object's surface. For this purpose, the surface is sampled with roughly uniform spacing, resulting in a finite set of points $\mathscr{P} = \{p_1, \ldots, p_n\}$, $p_i \in \mathbb{R}^3$ consisting of n points [3].

The matching of two objects is done by finding for each point p_i on the target shape (the unknown object) the best matching point q_j on the reference shape (the known object from a catalogue). SCs provide a description for each

point. This description is relatively unique within the context of the parent object and it is easily comparable. To describe the object, the $n-1$ distance vectors from one point to all other sample points are used, which leads to a description of the object's shape relative to the reference point. According to [3] and [9], this is a rich description and when $n-1$ gets large, the description becomes exact.

Rather than using the full set of distance vectors, which provides a far too detailed description, the distribution of the vectors are used instead, in order to serve as a robust and compact way to achieve a highly discriminative descriptor [3]. For a point p_i on the shape, a coarse histogram of the relative distances between p_i and the $n-1$ remaining points is computed. This histogram is defined to be the Shape Context of the Basis Point (BP) p_b.

The histogram of the SCs, shown in 2, was successfully used in former studies, [2] for 2D and in [9, 6] for 3D. The 3D-SC is of a spherical shape and with bins in the elevation and azimuthal direction linearly divided (see Fig. 2), the 2D histogram is the equatorial section of the 3D histogram.

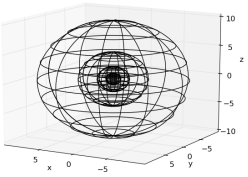

Figure 2: *3D histogram for Shape Contexts*

The log-polar bin pattern allows to describe the near neighbourhood of a BP more precisely, whereas the points more far away are combined in larger bins, coarsely describe the overall context of the object's shape with respect to the BP.

As this form of description is based on relative distance information, its invariance against translation is intrinsic. By normalizing the vectors with the BP-to-point distances, invariance against scaling can be achieved as well. To achieve rotational invariance, a relative reference frame for each SC can be used [3, 6].

The SCM follows the paradigm of feature vectors, where SCs are used as intuitive feature vectors [9]. This allows to describe the similarity between two SCs as their vicinity in the multidimensional feature space. By relying on feature vectors, the matching can be sped up by using advanced methods which help to reduce the search space dimensionality, e.g. clustering similar vectors or reducing the dimensionality of the vectors [9]. Also locality-sensitive hashing has been proposed to reduce the amount of required comparisons [6].

3.2. Generating shape contexts from DEM patches

SCs are used to describe DEM patches in order to make them comparable and to efficiently store the relevant information. Each patch is regarded to be a single 3D-object whose shape is defined by the single voxels of the DEMs, hence a patch is an already sampled 3D-object.

But it has to be considered that only the orbiter DEM provides approximately uniform sampling, whereas, due to the perspective nature of the camera system[1], the sample distance in the rover DEM increases with the distance to the point of view (see also section 2.1).

In contrast to the original SCs (see section 3.1) which describe a complete object with help of the $n-1$ BP-to-point distance vectors, the SCs in this work are more seen as feature descriptors, and this set of features describes the object itself. Based on this approach, N BPs are randomly chosen with a uniform distribution over the patch. Their surrounding area, i.e. their Basis Region (BR), is described with help of SCs (feature description) and the specific set of SCs and their appearance describes the patch itself (object description). The size of the BRs is usually smaller than the patch's one, but they can overlap as well.

The process of the Shape Context Generation (SCG) is as follows

1. Calculation of the histogram bin boundaries and the volume of each bin
2. Random selection of N BPs p_b from the patch data point set $\mathscr{P}_a$. The selection shall result in a uniform distribution of the BPs over the patch area.
3. Extraction of the BR, i.e. points within a certain distance to the BP
4. For each BP:
   (a) compute the surface normal vector of the BR through the BP
   (b) orient the histogram kernel in a way, that its polar axis is collinear with the normal vector, and its centre is the BP
   (c) Computation of the point density within a radius δ around each point $q_j \neq p_i$ in the BR
   (d) Computation of the BP-to-point distance vectors for all points in the BR
   (e) Allocation of the distance vectors to the corresponding bin
   (f) Each bin count is normalized with its point density ρ_i and the bin's volume $V(k,l,m)$

[1] Close objects cover many pixels within the 2D image, whereas far objects cover only a few pixels

3.2.1. Histogram bin boundaries

For the computation of the SC, a kernel of the same shape as shown in Fig. 2, is centred on a BP and it is oriented with its north pole on the surface normal vector $\vec{n}$ of the BR around the BP (see Fig. 3). In the radial direction, the kernel is divided in K logarithmically spaced bins with boundary positions at [6]

$$r_k = \exp\left\{\ln(r_{min}) + \frac{k}{K}\ln\left(\frac{r_{max}}{r_{min}}\right)\right\} \quad (2)$$

where $k = 0\ldots K \in \mathbb{N}$ is the index of the boundaries, $r_{max} = r_K$ is the outer radius of the kernel (and therefore the SC) and $r_{min} = r_0 > 0$ is the innermost boundary position with respect to the BP. The limitation of the lower radius to r_{min} shall avoid the SC to be excessively sensitive to small variations close to its centre [6]. The divisions in the elevation direction are given by

$$\theta(l) = \frac{l\pi}{L}, l = 0\ldots L \quad (3)$$

,

whereas the boundaries in the azimuthal direction are calculated with

$$\varphi(m) = \frac{m2\pi}{M}, m = 0\ldots M \quad (4)$$

.

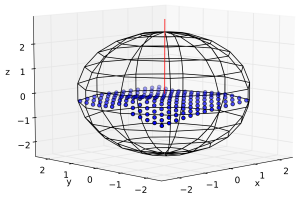

Figure 3: *Basis region data points with centred and correctly oriented histogram kernel (only outer boundary shown)*

3.2.2. Surface normal vector for rotation invariance

A local least square fitting approach by [18] was used to determine the normal vector of the surface in the BP. A possible alternative is the RANSAC algorithm by [5]. The normal vector represents the z-axis of the BR's reference frame with the BP being its origin and all distance calculations are performed in this frame.

3.2.3. Bin counts and normalization

The histogram h_i of BP p_i represents the distribution of the BP-to-point distances, expressed as [6]

$$h_i(k,l,m) = \#\left\{q_j \neq p_i : \left\|q_j - p_i\right\|) \in bin(k,l,m)\right\} \quad (5)$$

where $\|\cdot\|$ is the Euclidean distance in the $\mathbb{R}^3$ and q_j is the j-th point in the BR with $j = 0\ldots n-1$. The bin count for a point q_j is weighted with the factor $w(q_j) = \frac{1}{\rho_j \sqrt[3]{V(k,l,m)}}$ in order to account for the large differences in the bin volume $V(k,l,m)$, and differences in sampling density, with ρ_j representing the density of adjacent points that are within a radius δ around q_j.

3.3. Shape Context Matching

The SC-based descriptions of the rover patches and the orbiter patches are stored in two catalogues were each patch is represented by its own set of SCs. To determine the similarity between two patches, their matching costs are computed following the representative descriptor method from [6]. For each rover patch BP p_i a query on the orbiter patch catalogue is performed to find its complement BP q_j with the lowest matching costs. First the feature space distances between the SCs of the two patches under comparison are computed. Second, the sum of the n minimum distances determines the matching costs for one patch:

$$C_{i,j} = \sum_{j\in\{1,\ldots,N\}} \min_{i\in(1,\ldots,I)} \left\|q_j - p_i\right\| \quad (6)$$

The patch pair with the lowest matching costs $C_{i,j}$ represents the best match.

4. MATCHING EXPERIMENTS

In order to show the feasibility of the described SCM for the registration of DEM patches, experiments with a simulated, virtual Mars surface were conducted. This approach allowed to carry out the experiments in a completely controllable environment, in terms of ground resolution and additional details that could be added to the model. The Mars surface models were achieved with the software ExoSim by Stefan Kral [2], which is described in [10].

In total, two experiments were carried out. First, the matching of several patches but with additional small details, such as rocks and topographical variations, in the rover DEM, in order to determine how such a more realistic surface would affect the results (section 4.3). And second, by using orbiter DEMs with different ground resolutions, the robustness of the matching implementation against resolution differences was tested (section 4.4).

As the main output, the matching ratio, i.e. the ration between successful matches and the total amount of possible, correct matches was computed for each experiment.

4.1. Input data for the experiments

A 256×256 m cut-out of an original DEM of the Mars surface taken by the HiRISE camera was used as the un-

[2] `http://redfibre.net/orbital/projects/exoplanet/`

derlying raw data for the surface model. The DEM-cut-out, as shown in Fig. 4, is situated at the Husband Hill area close to the "Homeplate", where the MER Spirit was positioned during the Martian winter of 2006 (see Fig. 4a). The horizontal resolution of the original DEM [19] is 1 m whereas the vertical resolution is in the range of some decimetres [24].

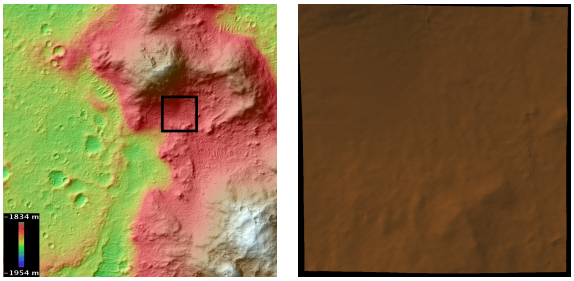

(a) *Colour coded elevation map of the Husband Hill region on Mars. The location of the used DEM cut-out is shown as a square.*

(b) *Bird eye's view of the resulting virtual Mars surface model with a horizontal ground resolution of 0.26 m/pixel.*

Figure 4: *Height elevation model of the original DEM, which was used to create the virtual* $256\,m \times 256\,m$ *Mars surface area. Fig. 4a is based on image material from NASA/JPL/University of Arizona/USGS [19].*

With help of a linear interpolation, the horizontal ground resolution of the model, shown in Fig. 4b, was increased to 0.26 m/voxel, which was necessary to allow the addition of so called height noise. This is an additional height profile which gives the surface model a more realistic appearance, as topographical details such as small bumps or sinks, which are not available in the raw DEM, can be added. The height profile is achieved with help of a fractal noise function (Perlin noise), which is usually used in image synthesis to achieve a realistic appearance of natural phenomenons, e.g. topology, clouds or water [20, 21]. The effects on the data set are shown in Fig. 6, were the increase of small occlusions becomes visible in the DEM with added height noise. Furthermore, rocks of different sizes can be distributed over the model (see Fig. 5c). These addition were only used for the rover view, in order to introduce small occlusions as they are apparent in reality, too.

As input data, XYZ-maps resulting from rendered views of the model are used. Such maps are produced when registering a pair of stereo-images in preparation of the DEM-generation, hence they are available as a side product. The XYZ-maps were read out of the rendered views of the surface model, e.g. the orbiter-map was derived from a bird's eye view on the model. For the second experiment, the orbiter-map's resolution was decreased by sub-sampling it, i.e removing points.

The rover-map simulates the mast-height of a small rover with the point of view being 1.2 m above the ground at the current position. As it can be seen from Fig. 5, a small hill is in front of the rover, resulting in a large occluded area within this data set. This view was chosen, in order to determine how well the matching procedure deals with large occluded areas. Unlike real DEMs from stereo-vision data, the depth accuracy in the experiments did not decrease with the distance to the view point.

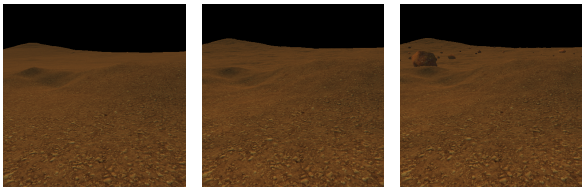

(a) *Same details as in the orbiter view*

(b) *With additional details from height noise*

(c) *Height noise and rocks of different sizes*

Figure 5: *Rover views on the model with different levels of detail. Images by Stefan Kral.*

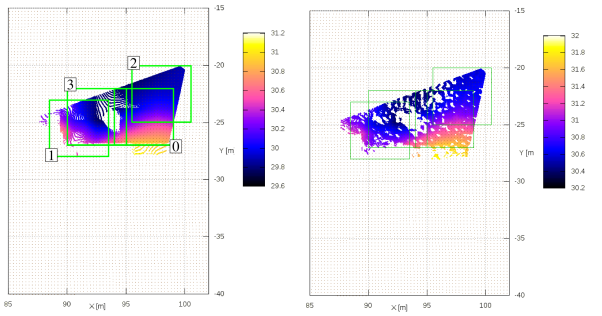

(a) *Without height noise and numbered rover patches*

(b) *With additional Perlin height noise*

Figure 6: *Effects of Perlin height noise on the rover-XYZ-map, here the non-occluded part directly in front of the rover point of view is shown. The rover data points are colour coded with respect to their z-value (elevation), whereas the orbiter-points are shown in brown. The height noise adds additional small occlusions to the rover data set. Also the difference in sampling uniformity between rover- and orbiter data sets becomes visible. The patches for the rover patch catalogue are bordered in light green.*

4.2. Patch selection and Shape Context Generation

As the experiments were intended to test the feasibility of the SCM for DEM patch matching and in order to have more control about the specimen, the patches were selected by hand. For the experiments a best case scenario regarding the patch location and orientation was assumed. Hence, the orbiter- and rover patches were chosen to be aligned, of the same size and at the same position, i.e. completely overlapping.

Four patches were chosen from both data sets, within the field of view of the rover-map (see Fig. 6a). The rover patches of this selection were mostly within the

rover-FOV, contained larger areas of occlusion and were overlapping, which was intended to use as a check on how well the SCM can distinguish between patches with nearly similar data.

Additionally, to enlarge the orbiter patch catalogue and in order to check if mismatching only happens with close-by or overlapping patches, four more patches were chosen from the orbiter-map outside of the rover's field of view.

Each patch covered an area of $5m \times 5m$ and it was described by 20 SCs which were centred on uniformly distributed, randomly chosen BPs. The parameters used for the SCG are given in Tab. 1.

Table 1: *Parameters for the Shape Context Generation of Experiment 1 and 2*

Parameter	Value	Unit
Width of a patch w_{patch}	5	m
Number of basis points per patch	20	
Minimum histogram radius r_{Min}	0,3	m
Maximum histogram radius r_{Max}	2,5	m
Number of radial divisions r	10	
Number of divisions in elevation directionθ	12	
Number of divisions in azimuthal direction φ	12	
Radius δ for the point density around sample points	1	m
Investigated ground resolutions of the orbiter DEM (only experiment 2)	0.26; 0.78; 1.04; 1.30; 1.57	m/voxel

4.3. Experiment 1 - Rover DEM with different levels of detail

The intention of the experiment was the investigation of the effect that small occlusions in the rover data can have on the matching performance. For this, three rover views with different levels of detail were used (see Fig. 5). First, the unaltered rover data (low level of detail), second rover-data with additional height noise (medium level of detail) and third, rover data with height noise and randomly distributed rock models of different sizes (high level of detail). The orbiter view remained unaltered and had a horizontal ground resolution of 0.26 m/pixel. For each level of detail, 10 runs were completed, each of them consisting of the following steps:

- random selection of 20 BPs in each patch
- calculation of the SCs for the selected BPs and storage in the corresponding catalogue
- computation of the cost matrices for each rover-to-orbiter patch combination (32 possible pairs with 400 SC comparisons per patch combination)
- selection of the patch match with the lowest matching costs
- computation of the matching ratio

The overall matching ratio per level of detail was computed as the average of the 10 matching ratios of the single runs.

4.4. Experiment 2 - Different ground resolutions of the orbiter DEM

Experiment 2 was intended to show the matching behaviour for different horizontal ground resolutions of the orbiter DEM. Five different resolutions, ranging from 0.26 m to 1.57 m, were investigated, using the same parameters as for experiment 1 (see Tab. 1). To achieve the different resolutions, only each $x-th$ point of the orbiter data was used. The rover input data consisted of the low level of detail rover-view, i.e. this test was only investigation the robustness against differences in resolution.

For each resolution, five test runs, with the similar procedure as in experiment 1, were completed. The overall matching ratio per resolution was computed as the average of the 5 corresponding runs.

5. RESULTS

The results of experiment 1 are shown in Tab. 2. The amount of mismatches is highest with the medium level of detail, and only for this data set patches outside the rover FOV caused mismatching. The mismatches within the FOV were mostly caused by sections 1 and 3 (see Fig. 6a). Approximately 2/3 of the area of rover patch 1 is covered by points, and additionally this part is also largely overlapping with patch 3.

Table 2: *Resulting performance of the SCM at different levels of details of the rover view as found with experiment 1*

Level of detail	low	medium	high
Mean detection ratio (after 10 runs)	92,5%	75%	90%
Amount of mismatches	3	10	4
Mismatch with patches within the rover FOV	3	7	4
Mismatches with patches outside the rover FOV		3	

The results for experiment 2 are shown in Fig. 7 with a mean detection ratio of 85 % for the best resolution, 0.26 m and 0.05 % for 1.30 m. For all other resolution, no matching was achieved.

6. DISCUSSION

The results of both experiments show that it is possible to use SCM for the matching of DEM patches. Further-

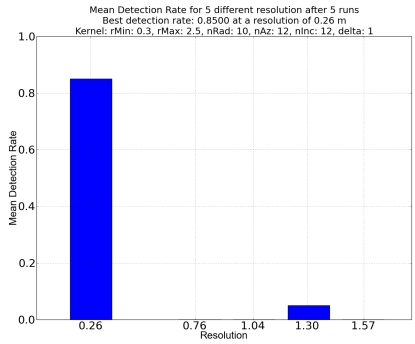

Figure 7: *Mean detection ratio for matching with orbiter DEMs of different horizontal resolution.*

more, experiment 1 showed that mismatching mainly occurs with patches that are mostly similar, as it was the case for patch 1 and 3 which caused most of the mismatches. Experiment 2 revealed, that the current implementation of the SCM is not yet robust against resolution differences in the two datasets. As a workaround, it might be feasible to reduce the rover DEM's resolution with help of a blurring filter in order match the resolution of the two DEMs.

7. CONCLUSION

In this paper a new procedure for rover self-localization based on the matching of patches from rover and orbiter DEMs was proposed. The basic framework of this new method was introduced and as a first step in the development, as well as a proof of concept for the matching, Shape Context Matching was implemented after it had been identified as the most suitable approach. First experiments were carried out with help of a simulated Mars surface and despite the basic implementation the results show the general feasibility of the SCM for the matching of DEM patches. Nevertheless, the proposed self-localization framework as well as the presented matching implementation still require further enhancements before a final statement about its usability for a reliable and accurate self-localization can be made. Regarding the advantage of reusing already available image data and because a complex identification and extraction of landmarks is not required, the author proposes a further investigation of this self-localization approach in order to enable more autonomous rovers in the future.

ACKNOWLEDGEMENTS

This work is based on my final thesis [15] in the program of Aerospace Engineering at the Technical University of Berlin. I would like to thank Prof. Dr.-Ing. Klaus Brieß for the supervision of this thesis. The work itself was carried out at the DLR - Institute of Planetary Research with support of Dipl.-Inf. Frank Trauthan, whom I would like to thank for the mentoring and the help during my thesis. Finally, I would like to thank Stefan Kral, for the provision of the simulated Mars surfaces as well as for many fruitful discussions.

REFERENCES

[1] S. Belongie and J. Malik. Matching with shape contexts. In *Proceedings IEEE Workshop on Content-Based Access of Image and Video Libraries 2000*, pages 20–26, Hilton Head Island, SC , USA, 2000. IEEE Comput. Soc. 3

[2] S. Belongie, J. Malik, and J. Puzicha. Shape context: A new descriptor for shape matching and object recognition. In *Proceedings of NIPS 14, Neural Information Processing Systems 2000*, pages 831—-837, Vancouver, B.C., Canada, 2000. Citeseer. 3, 4

[3] S. Belongie, G. Mori, and J. Malik. *Matching with shape contexts*, chapter 4, pages 81–105. Birkhäuser Boston, Boston, 1 edition, 2006. 3, 4

[4] G. Chin, S. Brylow, M. Foote, J. Garvin, J. Kasper, J. Keller, M. Litvak, I. Mitrofanov, D. Paige, K. Raney, M. Robinson, A. Sanin, D. Smith, H. Spence, P. Spudis, S. A. Stern, and M. Zuber. Lunar Reconnaissance Orbiter Overview: The Instrument Suite and Mission. *Space Science Reviews*, 129(4):391–419, May 2007. 1

[5] M. A. Fischler and R. C. Bolles. Random sample consensus: a paradigm for model fitting with applications to image analysis and automated cartography. *Communications of the ACM*, 24(6):381—-395, 1981. 5

[6] A. Frome, D. Huber, R. Kolluri, T. Bülow, and J. Malik. Recognizing Objects in Range Data Using Regional Point Descriptors. In *Proceedings of the European Conference on Computer Vision (ECCV)*, volume 1, pages 1–14, Prague, Czech Republic, 2004. 3, 4, 5

[7] A. E. Johnson. *Spin-images: a representation for 3-D surface matching*. Phd, Carnegie Mellon University, 1997. 3

[8] U. Köhler and R. Jaumann. HRSC - die hochauflösende Stereokamera, 2009. 1, 3

[9] M. Körtgen, G. J. Park, M. Novotni, and R. Klein. 3D Shape Matching with 3D Shape Contexts. In *Proceedings of The 7th Central European Seminar on Computer Graphics*, 2003. 3, 4

[10] S. Kral. *Konzept und Simulation für ein autonomes Multi-Rover-System zur planetaren Exploration*. Diploma thesis (not published), Technische Universität Berlin, 2011. 5

[11] S. Lacroix, a. Mallet, D. Bonnafous, G. Bauzil, S. Fleury, M. Herrb, and R. Chatila. Autonomous Rover Navigation on Unknown Terrains: Functions and Integration. *The International Journal of Robotics Research*, 21(10-11):917–942, Oct. 2002. 1

[12] R. Li, Y. Chen, S. He, L. Yang, and M. Tang. Rover Localization: Comparison between Bundle Adjustment-based and HiRISE Orbital Image-based Methods. In *Lunar and Planetary Institute Science Conference Abstracts*, volume 40, page 2208, 2009. 1

[13] R. Li, K. Di, A. B. Howard, L. Matthies, J. Wang, and S. Agarwal. Rock modeling and matching for autonomous long-range Mars rover localization. *Journal of Field Robotics*, 24(3):187–203, Mar. 2007. 1

[14] R. Li, F. Xu, L. H. Matthies, C. F. Olson, R. E. Arvidson, F. I. Design, and M. Orbital. Localization of Mars rovers using descent and surface-based image data. *JOURNAL OF GEOPHYSICAL RESEARCH*, 107(0):1–8, 2002. 1

[15] M. Lingenauber. *Implementierung und Analyse eines automatischen Matchingverfahrens für die Selbstlokalisierung planetarer Rover*. Diploma thesis, Technische Universität Berlin, 2010. 8

[16] M. Maimone, Y. Cheng, and L. Matthies. Two years of visual odometry on the Mars Exploration Rovers. *Journal of Field Robotics*, 24(3):169–186, 2007. 1

[17] J. N. Maki, J. F. B. III, K. E. Herkenhoff, S. W. Squyres, A. Kiely, M. Klimesh, M. Schwochert, T. Litwin, R. Willson, A. Johnson, M. Maimone, E. Baumgartner, A. Collins, M. Wadsworth, S. T. Elliot, A. Dingizian, D. Brown, E. C. Hagerott, L. Scherr, R. Deen, D. Alexander, and J. Lorre. Mars Exploration Rover Engineering Cameras. *Journal of Geophysical Research*, 108(E12):1–24, 2003. 3

[18] N. J. Mitra and A. Nguyen. Estimating surface normals in noisy point cloud data. *Proceedings of the nineteenth conference on Computational geometry - SCG '03*, pages 322 – 328, 2003. 5

[19] NASA, Jet Propulsion Laboratory, University of Arizona, and USGS. Mars Exploration Rover Landing Site at Gusev Crater (DTEEC_001513_1655_001777_1650_U01), 2010. 6

[20] K. Perlin. An image synthesizer. In *Proceedings of the 12th annual conference on Computer graphics and interactive techniques - SIGGRAPH '85*, pages 287–296, New York, New York, USA, 1985. ACM Press. 6

[21] K. Perlin. Improving noise. In *Proceedings of the 29th annual conference on Computer graphics and interactive techniques - SIGGRAPH '02*, page 681, New York, New York, USA, 2002. ACM Press. 6

[22] I. Rekleitis, J.-L. Bedwani, and E. Dupuis. Over-the-horizon, autonomous navigation for planetary exploration. *2007 IEEE/RSJ International Conference on Intelligent Robots and Systems*, pages 2248–2255, Oct. 2007. 1

[23] J. Tangelder and R. Veltkamp. A survey of content based 3D shape retrieval methods. In *Proceedings Shape Modeling Applications*, pages 145–156. IEEE, 2004. 3

[24] University of Arizona. HiRISE - About Digital Terrain Models, 2010. 3, 6